scientific reports

Check for updates

OPEN

Ultra-sensitive heterojunction double gate BioTFET device for SARS-CoV-2 biomolecules detection

P. Vimala[1]✉, A. Sharon Geege[3], N. Mohankumar[2], T. S. Arun Samuel[3], T. Ananth Kumar[4]✉, P. Suveetha Dhanaselvam[5] & I. Vivek Anand[3]

The persisting SARS-CoV-2 genetic mutation could unintentionally increase human transmission, mortality, and aggravation. Since no specific pharmaceutical therapies or vaccinations exist, rapid detection and successful treatment are essential for managing the COVID-19 pandemic. BioTFETs exhibit superior sensitivity and faster response times than bioFETs, which are more vulnerable to substantial subthreshold swing and short-channel effects. This article presents the Dielectrically Modulated-Double Gate-Heterojunction-Tunnel FET-based biosensor (DG-bioHTFET) specifically engineered to identify and detect the nucleocapsid protein and RNA biomolecules with specific permittivity (k) of SARS-CoV-2 biomolecules embedded in the nanogaps. At V_{gs} = 1.5 V, the proposed device achieves a drain current (I_{ds}) of 2.32×10^{-5} A/μm. At k = 5 and k = 3.64, the I_{ON}/I_{OFF} ratios are 3.550×10^5 and 3.403×10^5, respectively. The data suggest that the device exhibits increased sensitivity to biomolecules possessing elevated dielectric constants. It is feasible to design ultra-sensitive TFET biosensors as a bio-recognition unit, which offers the benefits of rapid label-free detection and high sensitivity. The device exhibits superior performance in terms of high drain current with enhanced sensitivity for precise biosensing applications.

Keywords Tunnel field effect transistor, SARS-CoV-2, Sensitivity, Double gate, Heterojunction

The COVID-19 outbreak is classified as a pandemic by the WHO, which attributes it to the SARS-CoV-2 due to the alarming increase in the reported instances of human infection. The RNA molecules of SARS-CoV-2 continuously experiences progressive genetic modifications. Turkey provided the primary SARS-CoV-2 genetic code to the Global Initiative on Sharing All Influenza Data (GISAID) on March 25, 2020. As of May 31, 2021, Turkey has contributed around 4000 sequences to the initiative. The country's SARS-CoV-2 virus diversification data provides insights into the virus's origin and its subsequent adaptation to other regions[1–5]. Typically, viral antigens are identified by collecting saliva and blood serum samples. However, for COVID-19, nasopharyngeal swab specimens are employed. The positive detection rate of nasopharyngeal swabs was significantly higher than that of oropharyngeal swabs, particularly in victims. The positive rate of male nasopharyngeal swabs was substantially greater than that of female swabs, particularly in outpatient cases. According to the results, it can be inferred that the agreement between saliva and nasopharyngeal swab (NPS) samples is equivalent when detecting SARS-CoV-2 RNA using Real-Time Polymerase Chain Reaction (RT-PCR). Hence, saliva is also recommended as a non-invasive sample for detecting COVID-19, as it yields satisfactory results[6–8]. Various laboratory diagnostic methods, like real-time polymerase chain reaction (PCR), rapid antibody testing, and Enzyme-Linked Immunosorbent Assay (ELISA), have made it easier and more accurate to diagnose COVID-19 quickly[9–12].

Figure 1 illustrates the SARS-CoV-2 biomolecules genomic sequence. SARS-CoV-2 complete genome has a polyprotein that has approximately 7096 residues in length. This polyprotein is composed of various structural and non-structural proteins (NSPs). The genome of a virus is made up of two non-structural proteins called

[1]Electronics and Communication Engineering, Dayananda Sagar College of Engineering, Bengaluru, India. [2]Symbiosis Institute of Technology, Nagpur Campus, Symbiosis International (Deemed University), Pune, India. [3]Electronics and Communication Engineering, National Engineering College, Kovilpatti, India. [4]Computer Science and Engineering, IFET College of Engineering, Villupuram, Tamilnadu, India. [5] Electronics and Communication Engineering, Velammal College of Engineering & Technology, Madurai, India. ✉email: ervimala@gmail.com; tananthkumar@ifet.ac.in

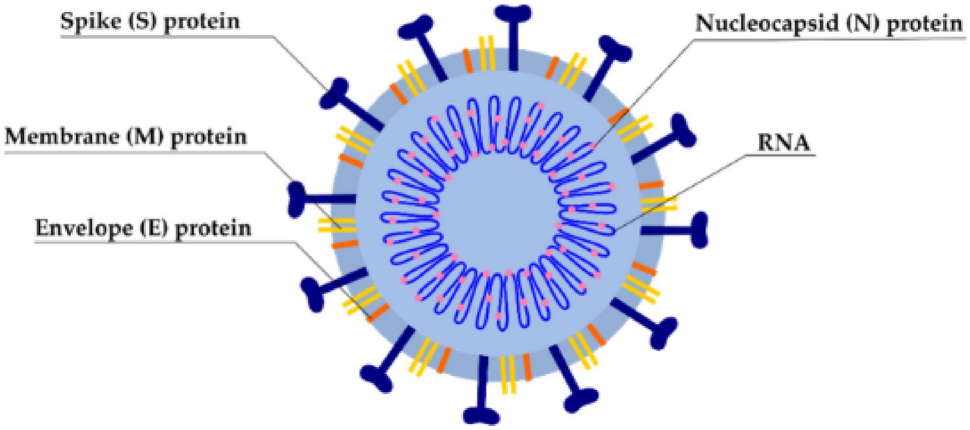

Fig. 1. Genomic sequence of SARS-C0V-2 virus[8].

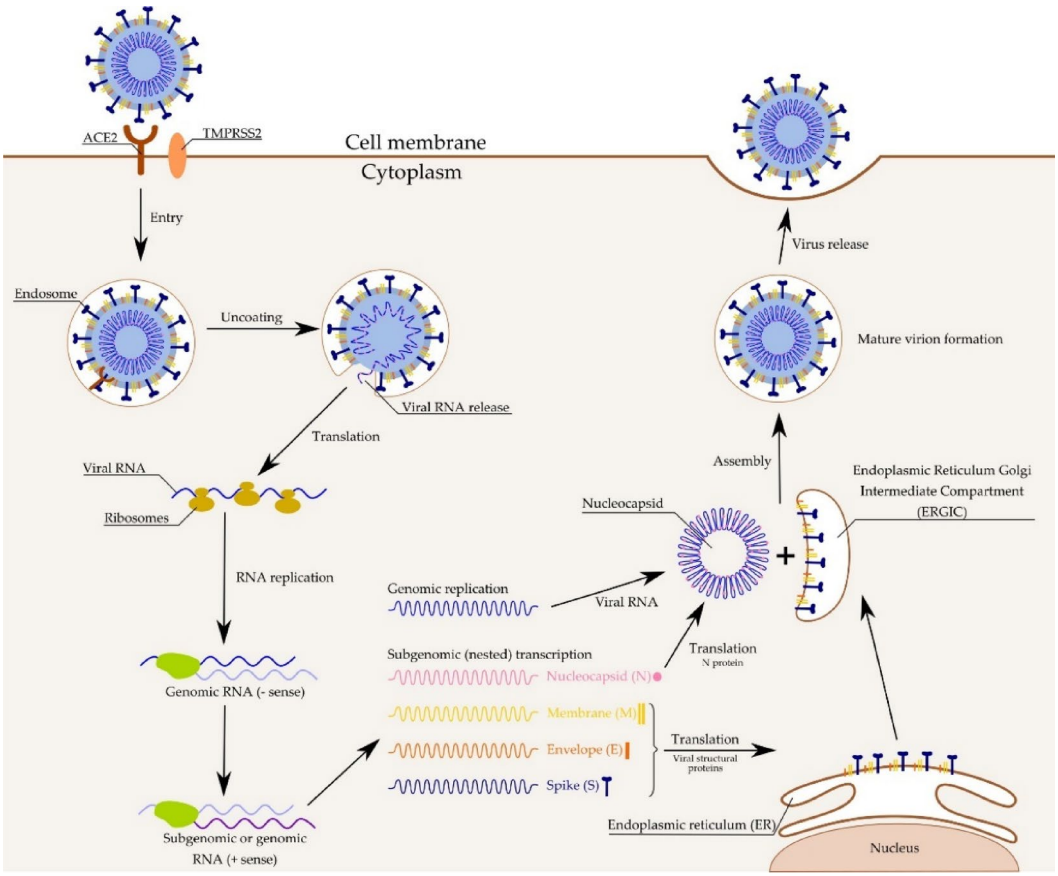

Fig. 2. Life cycle of SARS-CoV-2[8].

ORF1a and ORF1b. These proteins hold the nucleotide material. Then, the structural proteins follow these proteins. Moreover, the virus's RNA is synthesized to create complementary DNA (cDNA), which is eventually duplicated by polymerization of DNA. SARS-CoV-2 genome is a 29.8 kb positive-stranded RNA. This genome includes signals that encode four structural proteins, namely spike glycoprotein (S), envelope (E), matrix (M), and nucleocapsid (NC). Out of all the proteins, only the spike (S) glycoprotein is exposed on the exterior surface of the virus. This protein is highly immunogenic, meaning it triggers a strong host immune response. It is also the most reliable biomarker for diagnosing SARS-CoV-2 infection. The use of RNA, a template, is essential in cDNA synthesis. When DNA attains a specific temperature, it undergoes the process of denaturation, which causes to divide the two strands[13–15]. Figure 2 illustrates a SARS-CoV-2 life cycle inside a host cell, which include

entering into the host cell, releasing RNA, synthesizing proteins, assembling the virus, and releasing new viral particles.

Among the diagnostic methods that are currently available, FET-based biosensors are a promising candidate due to their high sensitivity, which enables instantaneous measurements with minimal analyte quantities. These biosensors have significant possibilities for on-site detection, point-of-care testing, and clinical diagnosis. The bio-FET is further classified into ion-sensitive FETs and enzyme-based FETs. ISFETs adhere charged molecules between the gate dielectric and the ionic solution to modify their electrical properties. ISFETs are sensitive to charged biomolecules and fail to detect uncharged biomolecules[16–20]. Enzyme-based BioFETs are frequently used for detecting antigens, whereas specifically built BioFET platforms are applied in fast viral antigen assays. Moreover, the development of two-dimensional material-based field effect transistors enables the detection of viral biomarkers without the need for labeling. Electrical double-layer-gated BioFETs test artificial saliva for COVID-19[21]. BioFETs confirm faster shifts with an optimal detection limit for SARS-CoV-2 nucleocapsid protein around ≈3 pM[22]. FET-based biosensors experience challenges with scaling limits, such as higher subthreshold swing (SS) and short-channel effects (SCE). In contrast, biosensors based on tunnel field effect transistors (TFETs) can provide superior performance and sensitivity with a faster response time as tunneling mechanism results in low subthreshold swing and reduced leakage. Nevertheless, achieving abrupt junctions in a TFET is a considerable challenge, as they are crucial for facilitating tunneling.

These devices are well-suited for biosensing applications due to their high sensitivity and minimal power consumption. Moreover, they can detect viral components without labelling, making it an attractive biosensing option and also distinguishes infected and control samples for accurate diagnostic testing. Graphene based TFETs provide the advantages of electrostatic gating and functionalization using antibodies or aptamers to achieve high sensitivity and conductivity. Direct viral protein identification makes this technique effective to identifying clinical sample SARS-CoV-2[23–26].

This research describes the development of a biosensor called label-free Dielectric modulated Double Gate Heterojunction Tunnel field-effect transistors (DG-bioHTFET) for quick and accurate identification of SARS-CoV-2 biomolecules. Incorporating heterojunction in TFETs helps to enhance tunneling efficiency, improve ON current, reduce leakage current, enhance ION /IOFF ratio, and have the flexibility to utilize versatile materials in source and channel/drain regions[27–30]. This biosensor has remarkable sensitivity and possesses the capacity to identify the SARS-CoV-2 biomolecules by monitoring drain current variation (I_Ds) for viral detection. The primary benefits of the TFET-based biosensor include simple fabrication and rapid sensing response with the ability to obtain dynamic real-time responses using inexpensive digital readers that can be adjusted for various applications[31–34]. A new GaAs/GaSb polarity-controlled tunnel field-effect transistor (PC-TFET)-based biosensor with ultra-high sensitivity is reported in[35]. Due to its fabrication complexity, the sensor is not a promising option for biomedical applications. In our proposed device architecture, the fabrication processing steps are simpler, making it feasible for biomedical applications. The experimental data from a conventional TFET in reference[36] is utilized to calibrate and benchmark the parameters of our proposed device model to be simulated. It is performed following the integration of all dimensions and device bias conditions. The I_{ds}-V_{gs} of the proposed TFET biosensor closely approaches the values previously depicted in Fig. 3.

Proposed device structure and specifications

Figure 4 depicts the two-dimensional view of a Dielectrically modulated- double gate Heterojunction-bioTFET [DG-bioHTFET]. HfO_2 is used as an oxide material with a high dielectric constant (k = 25), providing good thermal stability and reduced leakage, improving the output characteristics (Ion) and efficiency. Better gate control over the channel is achieved by introducing a double gate architecture with aluminium as the ohmic contact. Asymmetrical doping is implemented in the p + source and n + drain regions to mitigate ambipolarity. Germanium and silicon are chosen as hetero materials for source and channel/drain, respectively, to improve the device's sensitivity. The SARS-CoV-2 biomolecules is too big to be fitted into a 5 nm BioTFET gap; instead, the device presumably detects smaller fragments such as nucleocapsid protein (~4 nm) or RNA (~2 nm) with specified permittivity. Our proposed work includes the concept of dielectric modulation, and the current varies with the permittivity of the biomolecules. Surface functionalization with bioreceptors (e.g., antibodies, aptamers) allows selective binding within the interstice. Targeting RNA, being extremely small, permits direct implantation.

In TFET, the doping concentration directly influences the bandgap energy. When there is a large concentration of dopant atoms, as is commonly found in source and drain regions, the interactions between the dopant atoms can cause a decrease in the bandgap energy. This is because the effective potential is shifted, influencing the state of electrons within the material. The impact is especially significant in the source and drain regions, where a high doping level is required to ensure effective carrier movement.

Table 1 shows the device specifications and its dimensions. Figure 5 illustrates the proper fabrication flow procedure for the Double Gate Heterojunction Tunnel FET-based biosensor. Table 2 summarizes the respective biomolecules and their dielectric constants. Under these circumstances, the sensing process takes place in an arid environment. The entire simulation is carried out in the Atlas Silvaco TCAD simulator.

Results and discussion

Performance characteristics of DG-bioHTFET

Figure 6 depicts the energy band diagram of the DG-bioHTFET. When the device is turned off, the tunneling current is minimal, and a substantial barrier prevents the flow of electrons from the source to the channel. It can be observed that there is a visible band bending (shown in the circle) near the center of the channel(~0.03 µm), where the tunnelling occurs. When a sufficient gate voltage is applied, the source material's conduction band

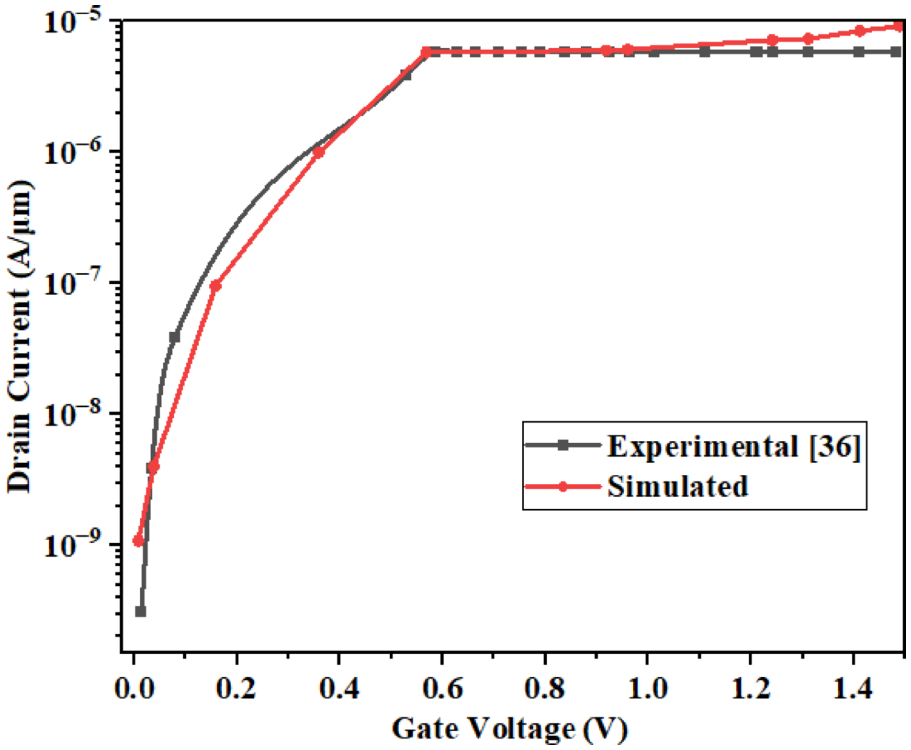

Fig. 3. Calibrated results of experimental TFET vs. proposed DG-bioHTFET.

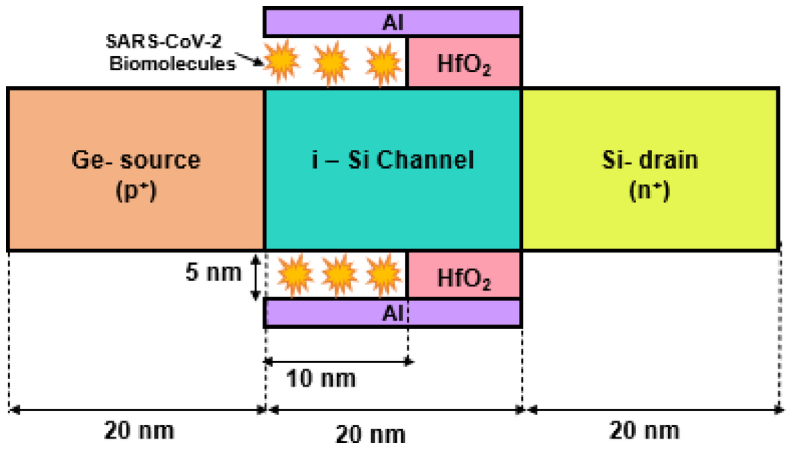

Fig. 4. Schematic cross-section of DG-bioHTFET.

S. No	Material specifications	Dimensions
1	Channel length, L_{ch}	20 nm
2	Source and drain length, L_S and L_D	20 nm
3	Nanogap length, L_{cavity}	10 nm
4	Nanogap thickness, t_{cavity}	5 nm
3	Metalwork function(aluminium)	4.2 eV
4	Source doping concentration	1×10^{19}
5	Channel doping concentration	1×10^{17}
6	Drain doping concentration	5×10^{20}

Table 1. Device specifications for the DG-bioHTFET-based SARS-CoV-2.

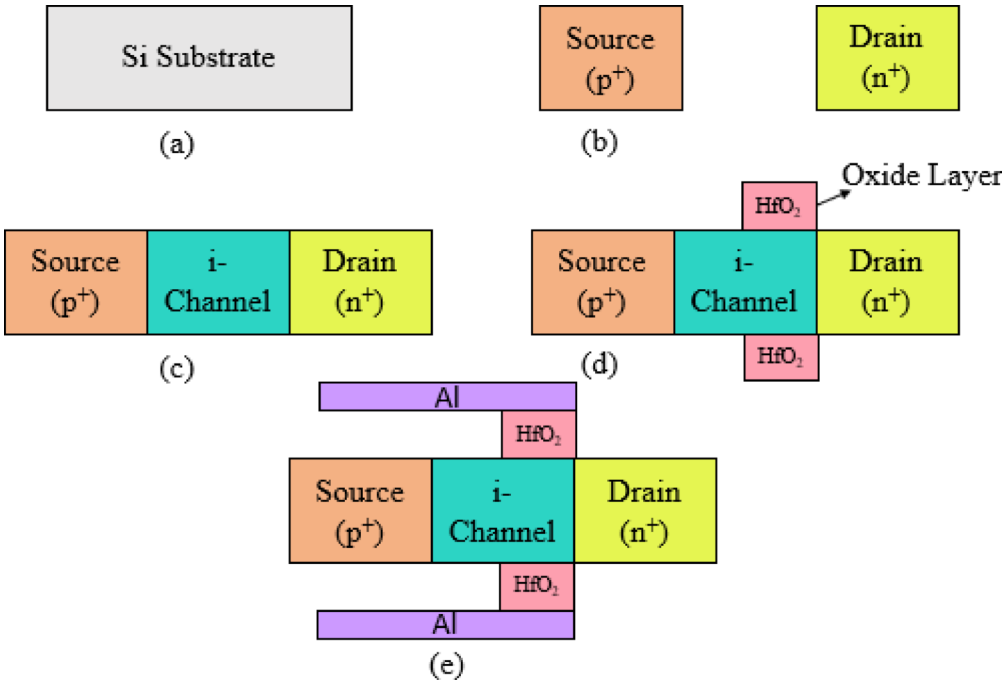

Fig. 5. Tentative fabrication flow process of Double Gate Heterojunction Tunnel FET based biosensor (a) Substrate (b) Masking & photolithography deposition of Source & Drain material (c) Deposition of Channel material (d) Formation of oxide Layer and etching to form nanogaps (e) Formation of metallic contact.

S. No	Biomolecules	High K-Value
1	Low-hydrated proteins	5
2	Glucose oxidase	3.64
3	Amino propyltriethoxysilan	3.57
4	Cholesterol oxidase	3.28
5	streptavidin/biotin	2.1
6	proteins/avian influenza	1.9

Table 2. Biomolecules and its dielectric constants are enumerated.

aligns with the channel material's valence band, which reduces the potential barrier width. Such alignment is vital for enabling efficient band-to-band tunneling and allowing current flow in TFETs. Higher ON currents in TFETs are directly attributed to this greater tunneling current. In addition, TFETs operate at lower supply voltages because of a reduction in potential barrier width during the ON state of the device. When k = 1(without biomolecule), the energy gap among them is 3.71 nm. Introducing the SARS-CoV-2 biomolecule (k = 5) decreases the energy band gap by 3.25 nm, which increases the tunneling current.

Figure 7 illustrates the variation of the surface potential across the channel length with the presence/absence of the biomolecule, in the nanogap at the source end beneath the gate. The presence of biomolecule (k = 5) causes a channel potential rise below the gate with increased permittivity compared to the absence of biomolecule (k = 1). The electrostatic channel potential is responsible for tunneling of more electrons from the Ge to Si interface. The potential barrier of Ge/Si is reduced, enhancing the tunneling of the electrons by increasing the tunneling current. Thus, the presence of the biomolecule can be detected from the elevation of the potential observed. The sharp rise in surface potential is due to the increased carrier concentration for SARS-CoV-2 biomolecule (k = 5) substantially increasing the drain current in comparison with the absence of biomolecule (k = 1). The SARS COV-2 biomolecules alter the carriers in the gate/channel interface providing high transconductance responsible for increasing the electrostatic potential.

Figure 8 displays the variations in the electric field along the channel length of DG-bioHTFET for k = 5, the presence of SARS COV-2 biomolecules represents a sharp peak visible at 0.02 μm, which indicates the high tunnelling probability with peak electric field in comparison with the absence of biomolecules (k = 1). The high surface potential leads to reduced bandgap allowing sufficient carriers to tunnel from source to the drain with reduced potential barrier and high ON current.

The biomolecules embedded in the nanogaps carrying the SARS-CoV-2 biomolecules exhibit peak electric field variations compared with air as the dielectric medium. Increasing the gate voltage modifies the surface

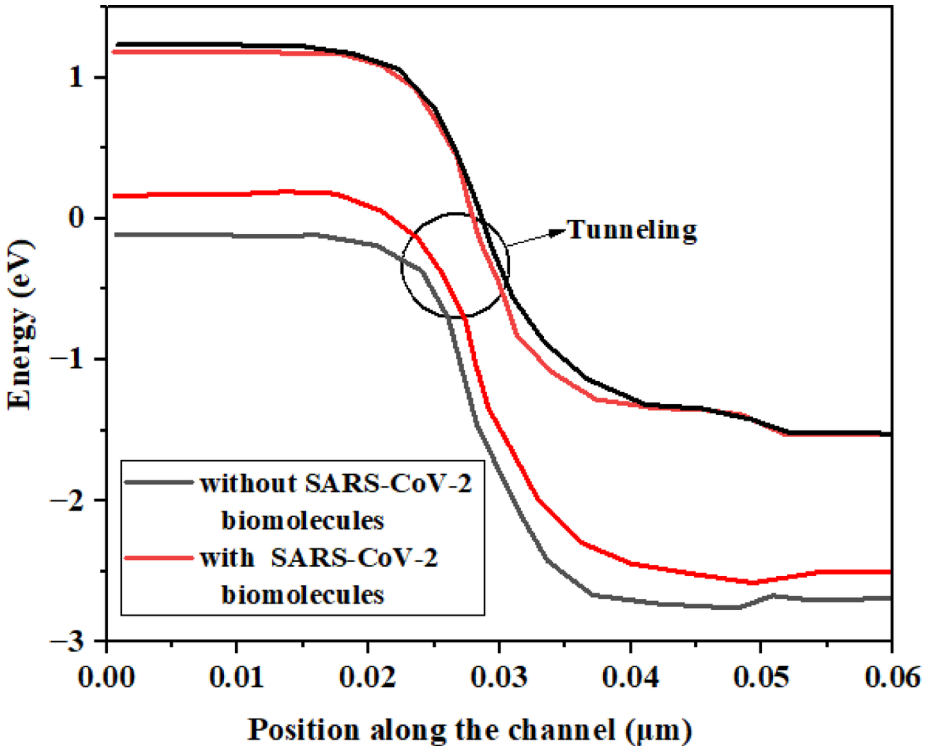

Fig. 6. Energy distribution(on-state) in label-free DG-bioHTFET.

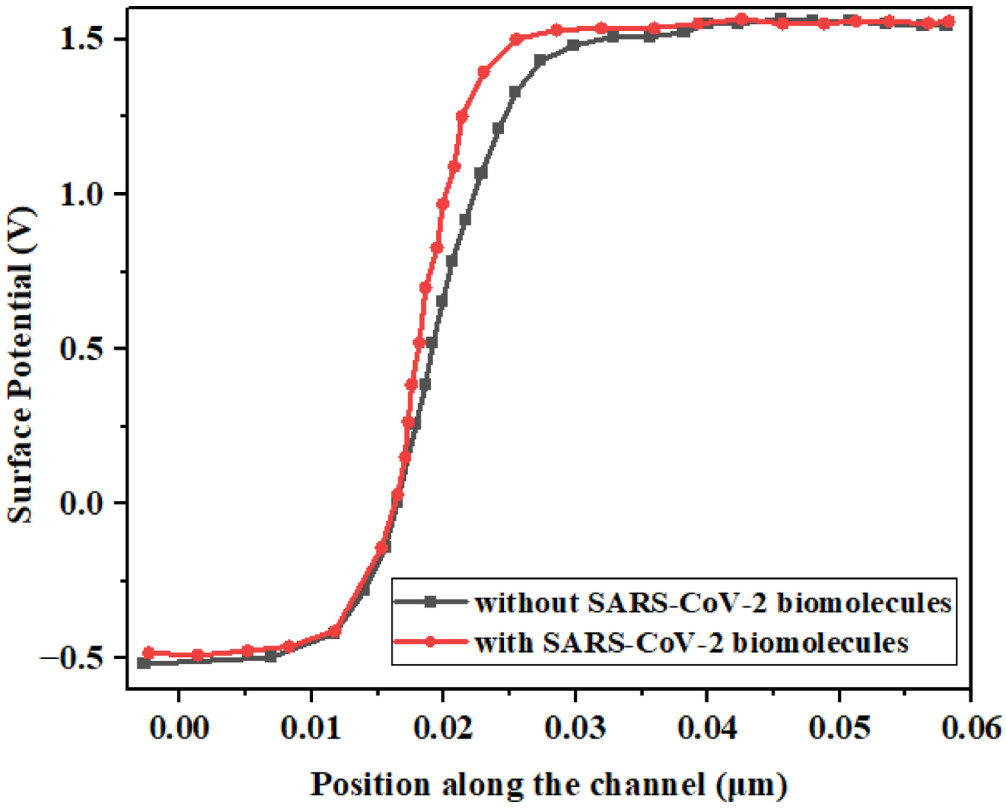

Fig. 7. Variation of potential across label-free DG-bioHTFET.

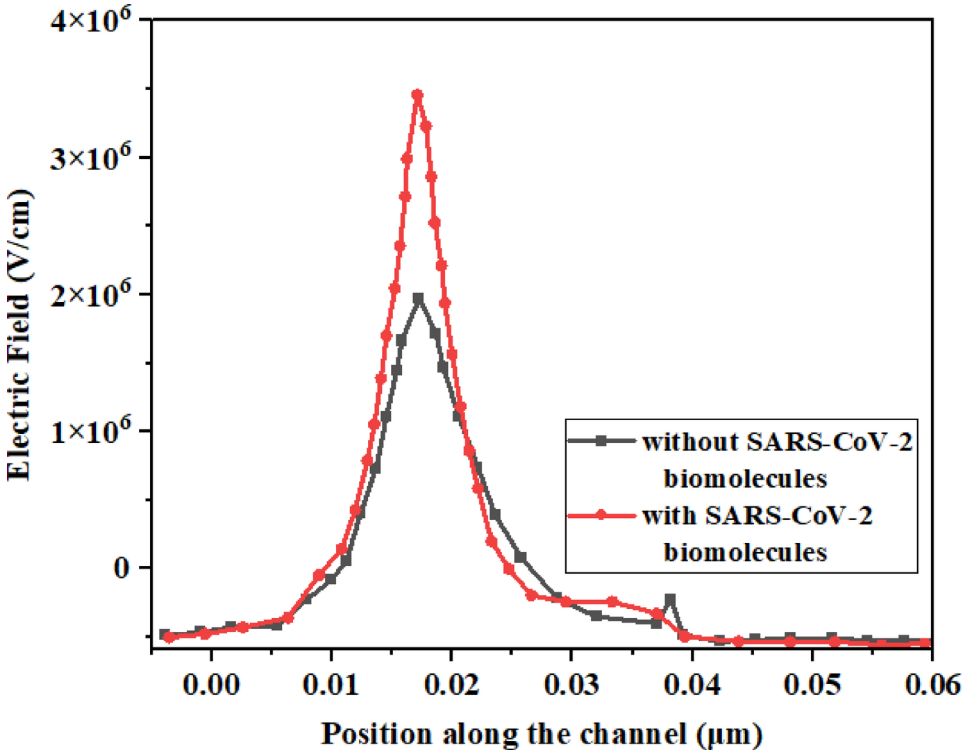

Fig. 8. Electric field variation across label-free DG-bioHTFET.

potential, directly enhancing the electric field in the channel. This form of modulation enables enhanced regulation of the electron tunneling process from the source to the channel, resulting in a higher drain current. The biomolecules embedded in the nanogaps (k = 5) carrying the SARS-CoV-2 biomolecules reaches a maximum value of 4×10^6 V/cm whereas the nanogaps containing air (k = 1) as a dielectric medium reaches a maximum value of 2.5×10^6 V/cm.Therefore, the variations in the electric field can determine the presence or absence of a biomolecule in nanogaps. The increasing number of electric field lines causes the accumulation of charges in the channel region.

As previous figures show, the biomolecules improves the band bending, surface potential and electric field. This speeds up the BTBT rate, which is the main conduction mechanism of TFETs. Hence, the current increases as more carriers tunnel from the source to the channel at lower gate voltages. Figure 8 displays the variations in drain current as the gate voltage increases without the biomolecule (k = 1) and with a biomolecule (k = 5). The drain current progressively increases as the gate voltage ranges from 0 to 1.5 V. Modifying the electric field is also essential in regulating the current flow by exploiting tunneling improvements. The sample containing the biomolecule exhibits a significantly higher current compared to the sample without the biomolecule. The drain current decreases in the absence of biomolecules and increases in the presence of biomolecules. The presence of a biomolecule in the cavity results in a high drain current of around 2.32×10^{-5}A, whereas the absence of a biomolecule (k = 1) leads to a lower current of around 1.13×10^{-7}A. Figure 9 shows the drain current variation across label-free DG-bioHTFET.

Figure 10 illustrates the variations in drain current induced by different bio-molecules within a single SARS-CoV2 virus particle. Ge-Si hetero material combination facilitates the optimization of band alignment, increasing the possibility of carrier tunneling. The biomolecules shown in the graph with different k-values exhibit a substantial variation in drain currents. By averaging these k-values, the ultimate current obtained for the virus sample is 2.32×10^{-5}A. Hence, the magnitude of the electric current flowing through the drain is crucial in detecting the SARS-CoV-2 biomolecules in pathological specimens.

Table 3 represents the performance analysis of the DG-bioHTFET device, examining several metrics such as surface potential, electric field, and drain current. The evaluation is performed for two distinct scenarios: one in the absence of a biomolecule and the other in the presence of the biomolecule.

Sensitivity analysis of DG-BIOHTFET

The effective gate capacitance increases, resulting in a significant shift in channel conductivity due to the biomolecules combination generated by the immobile receptors enclosed within nanogaps. As biomolecules fill the nanogaps, the drain current increases. SARS-CoV-2 drain current sensitivity is evaluated under the condition of k = air, demonstrating the absence of any biomolecules in the nanogaps. The drain current sensitivity is defined as follows,

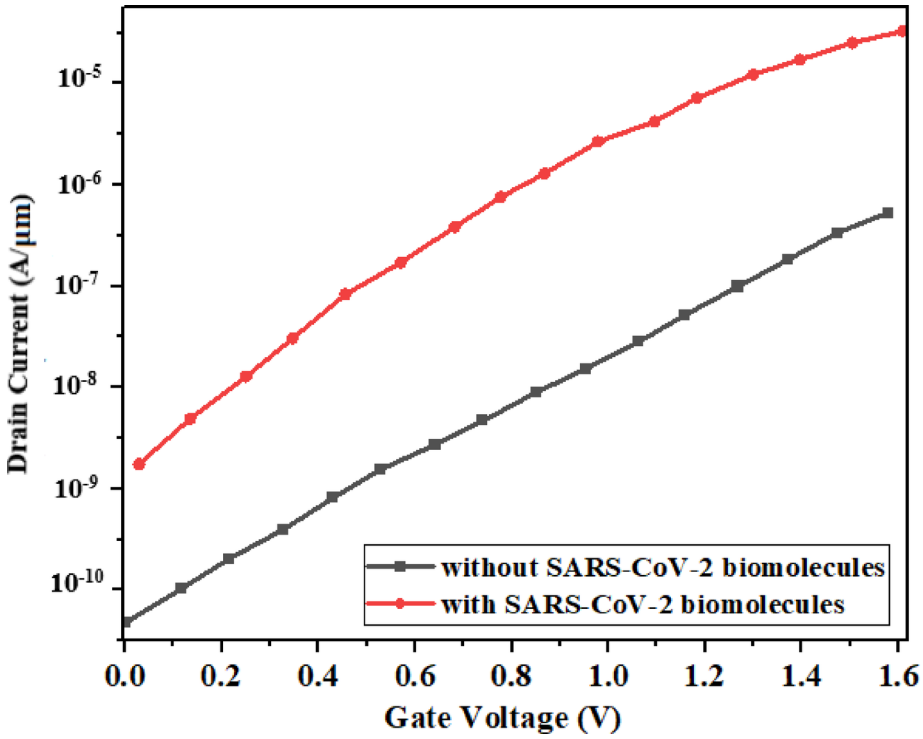

Fig. 9. Drain current variation across label-free DG-bioHTFET.

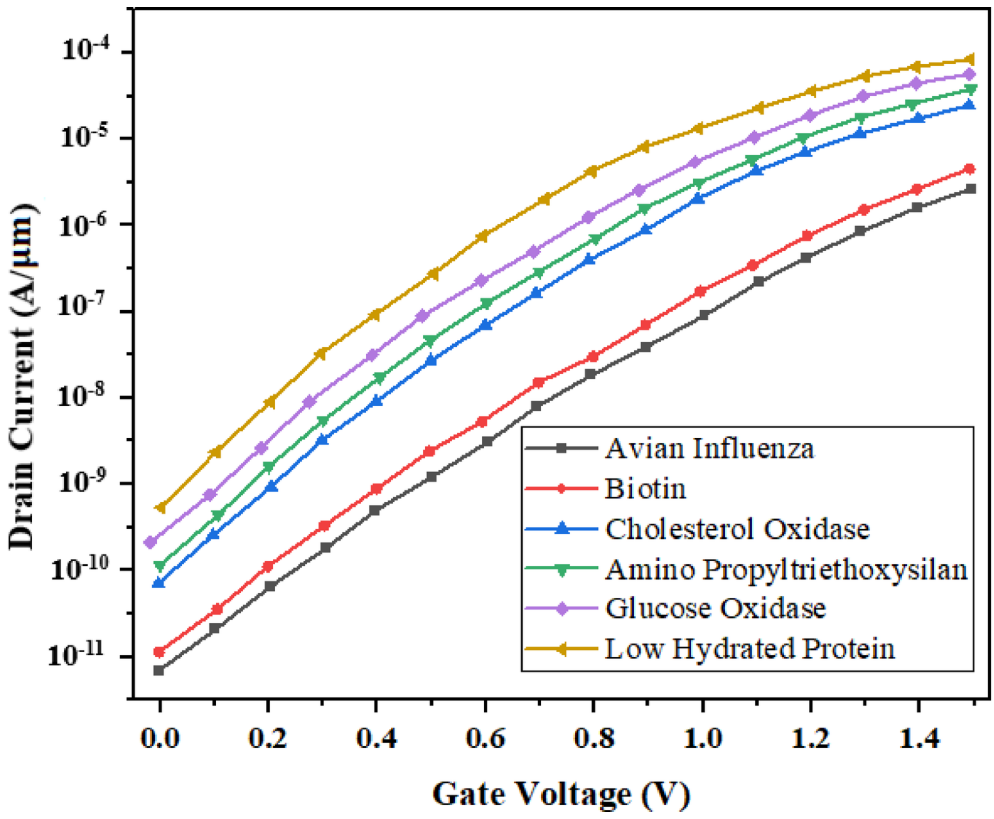

Fig. 10. Drain current variation for different biomolecules in label-free DG-bioHTFET.

Parameters	Without biomolecule	With biomolecule
Surface Potential (V)	1.49	1.48
Electric Field (V/cm)	2.5×10^{6}	4×10^{6}
Drain Current (A/μ m)	1.13×10^{-7}	2.32×10^{-5}

Table 3. Performance metrics comparison among without and with biomolecule.

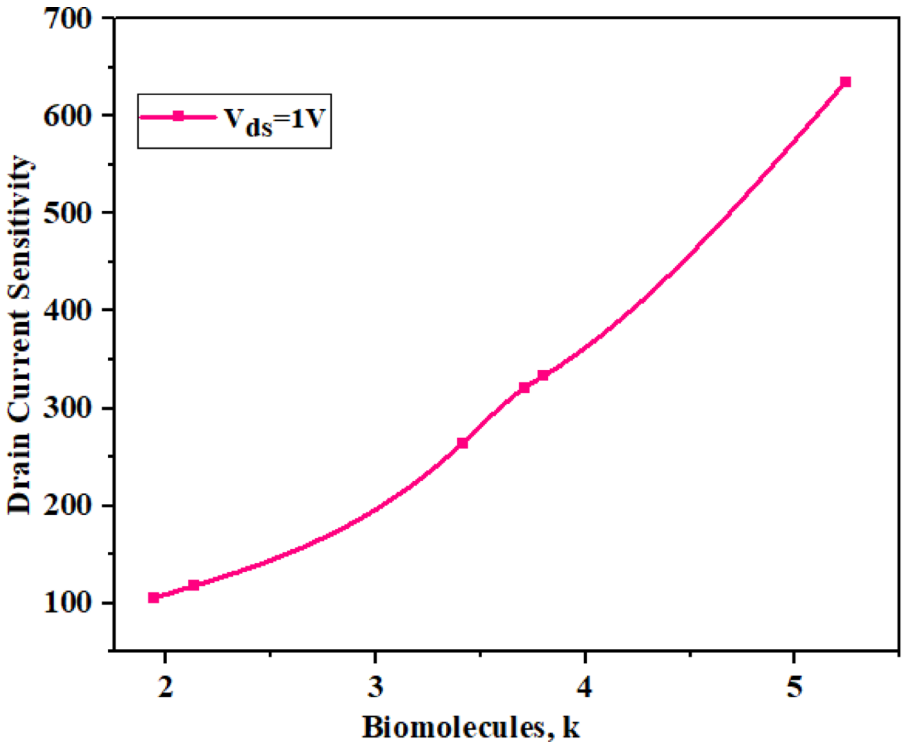

Fig. 11. Sensitivity analysis for various biomolecules in label-free DG-bioHTFET.

$$\text{Sensitivity} = \frac{I_{ds}\,(\text{bio}) - I_{ds}\,(\text{air})}{I_{ds}\,(\text{air})} \tag{1}$$

where,

I_{ds} (bio) represents the drain current in the presence of biomolecules in the nanogap

I_{ds} (air) is drain current reference with air as the dielectric, k = 1(absence of biomolecules)

Figure 11 depicts sensitivity analysis of various biomolecules in label-free DG-bioHTFET including germanium at the source-channel interface allowing the device to achieve sensitivity of about 635 at low hydrated proteins, which is higher than prior devices' sensitivity. The increased sensitivity of the proposed device architecture will be beneficial for other sensing applications. The sensitivity of this sensor depends on the charge density in DNA molecules. The ability of DNA molecules to store information makes these phenomena possible. It is reasonable to assume this will happen because DNA molecules can transfer charges. From the figure, it is evident that for biomolecules with higher permittivity(k = 5), the sensitivity is much improved, in contrast to biomolecules with lower k values, which are minimal when there is no presence of biomolecules.

Figure 12 shows the transconductance-gate ratio curves for different drain current values in label-free DG-bioHTFET. Every biomolecule results a separate $|g_m/I_{ds}|$ profile, because of its individual interaction with the channel or the gate of the proposed device. The ratio demonstrates the gate voltage effectiveness in controlling the drain current under specific circumstances, indicating the responsiveness of the biosensor. An increased transconductance to gate ratio contributes enhanced biosensor sensitivity by enabling the detection of biomolecule concentration. The increased sensitivity is crucial for applications in healthcare diagnosis as it impacts directly the device efficiency and response. A better $|g_m/I_{ds}|$ ratio is clearly shown for biomolecules with an increased k-value that are introduced into the cavity. At k = 5, the maximum $|g_m/I_{ds}|$ is attained for larger k-values. Biomolecules have an amplified controllability of the gate across the tunneling junction due to their raised k-value. As a result, $|g_m/I_{ds}|$ values are raised.

Figure 13 shows the drain-ON current sensitivity variations for different values of cavity length (L_{cavity}) The drain-ON sensitivity in DG-bio HTFET increases with the L_{cavity} and is maximum for 150 nm. For higher cavity

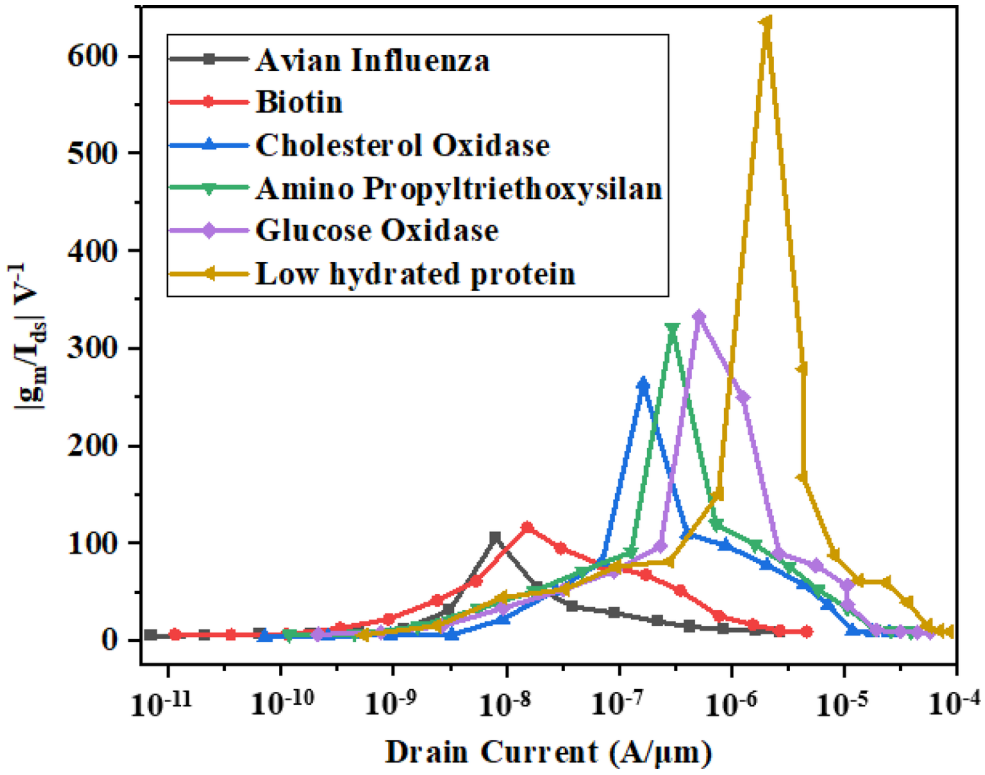

Fig. 12. Transconductance-gate ratio curves for different drain current values in label-free DG-bioHTFET.

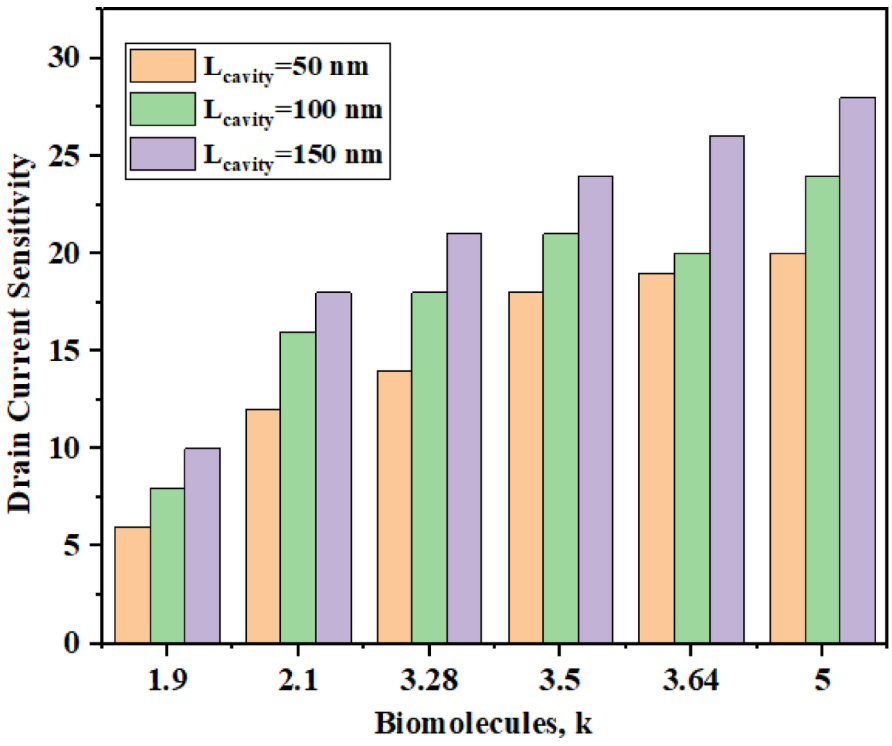

Fig. 13. Sensitivity variation for DG-bioHTFET against different k-values for cavity length variations in label-free DG-bioHTFET.

Bio- analytes	High-k value	I_{on}/I_{off} ratio
proteins/avian influenza	1.9	1.469×10^5
streptavidin/biotin	2.1	2.800×10^5
Cholesterol oxidase	3.28	2.875×10^5
Amino propyltriethoxysilan	3.57	3.171×10^5
Glucose oxidase	3.64	3.403×10^5
Low-hydrated proteins	5	3.550×10^5

Table 4. I_{ON}/I_{OFF} ratio analysis of DG-bioHTFET.

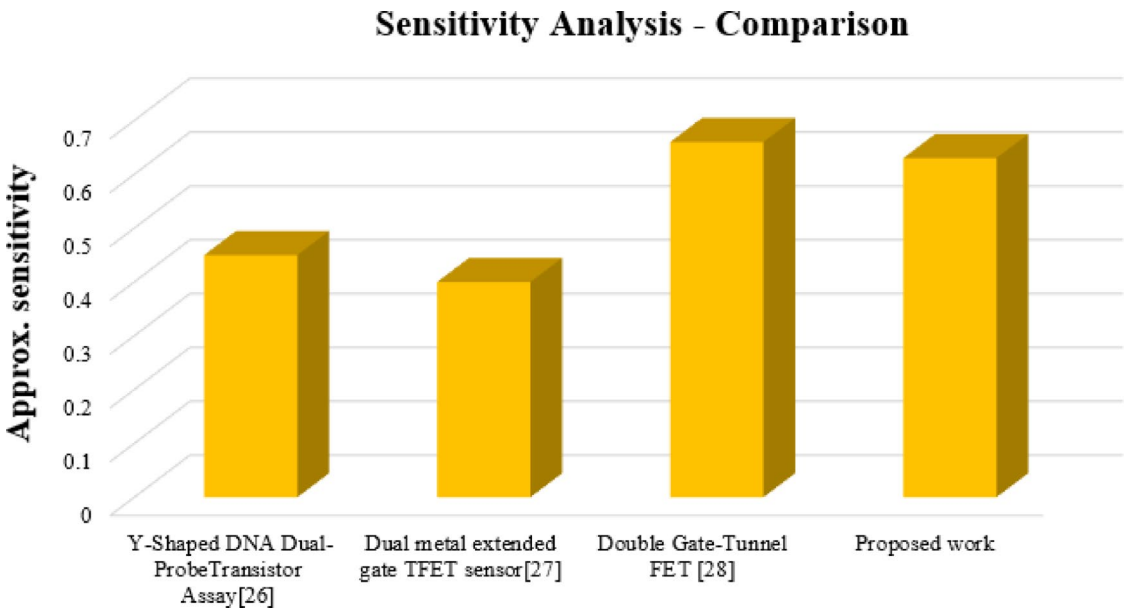

Fig. 14. Comparison of DG-bioHTFET sensitivity analysis with existing work.

lengths, the area for the interaction of biomolecules with the surface charges in the Ge barrier is significant with reduced height, thereby improving the tunnelling drain current with high sensitivity. Moreover, the device's sensitivity is low for biomolecules with low permittivity compared to those with high permittivity counterparts. The biomolecules with k = 5 exhibit higher gate control over the channel with reduced leakage, resulting in higher drain current in saturation regime, enabling fast and accurate prediction with improved sensitivity.

Table 4 depicts the ON and OFF current ratio of DG-bioHTFET for SARS-CoV-2 biomolecules. I_{ON}/I_{OFF} of Low-hydrated proteins (k = 5) obtained as 3.550×10^5. As the k-value goes from 1.9 to 5, the I_{ON}/I_{OFF} ratio shows an increasing trend. The I_{ON}/I_{OFF} ratio reaches its maximum at = 5 indicating that the device is more sensitive to biomolecules with higher dielectric constants and starts decreasing for low K values and reaches minimum with the absence of biomolecules.

Figure 14 presents a benchmark analysis of the proposed DG-bioHTFET for detecting SARS-CoV-2. The analysis primarily examines the sensitivity factor, whereas the phrase 'approx. sensitivity' is used in Fig. 13, which is taken from recently published research articles.

Conclusion

The primary goal of this research is to evaluate the biosensor's ability to detect a specific strain of SARS-CoV-2 using pathological samples. This research work analyzes and compares the impact of drain current and sensitivity on the performance of DG-bioHTFET for detecting label-free biomolecules with existing devices. This is investigated using Silvaco TCAD simulator. At V_{gs} = 1.5 V, the proposed device obtains a drain current (I_{ds}) of 2.32×10^{-5}A/μm. An increased transconductance-gate ratio enhances sensing capabilities, improving accuracy and reducing detection limits for biomolecular recognition. Dielectric modulation techniques significantly increase the transconductance-to-gate ratio. At k = 5 and k = 3.64, the I_{ON}/I_{OFF} ratio are 3.550×10^5 and 3.403×10^5 respectively. The values indicate that the device is more sensitive to biomolecules with higher dielectric constants. Overall, analysis demonstrates the potential and superiority of DG-bioHTFETs, rendering them suitable for high-precision biosensing applications.

Data availability

The datasets used and/or analysed during the current study available from the corresponding author on reasonable request.

Received: 5 October 2024; Accepted: 23 April 2025
Published online: 30 April 2025

References

1. Venkatesh, M. & Parthasarathy, P. Al_2O_3/ZrO_2 dual-dielectric Gr/CNT nanoribbon vertical tunnel FET based biosensor for genomic classification and S-protein detection in SARS-CoV-2. *Heliyon* **10**(9), e30077 (2024).
2. Mazin, A. et al. Carbon nanotube field-effect transistor (CNT-FET)-based biosensor for rapid detection of SARS-CoV-2 (COVID-19) surface Spike protein S1. *Bbioelectrochemistry*. **143** https://doi.org/10.1016/j.bioelechem.2021.107982 (2022).
3. Sreejith, S. et al. A comprehensive review on graphene FET bio-sensors and their emerging application in DNA/RNA sensingrapid Covid-19 detection. **206**. https://doi.org/10.1016/j.measurement.2022.112202 (2023).
4. Samson, R., Navale, G. R. & Dharne, M. S. Biosensors: frontiers in rapid detection of COVID-19. *3 Biotech.* **10**(9), 385. https://doi.org/10.1007/s13205-020-02369-0 (2020).
5. Esteban Piccinini, G. E. et al. Biofunctionalization of graphene-based FET sensors through heterobifunctional nanoscaffolds: technology validation toward rapid COVID-19 diagnostics and monitoring. **18** https://doi.org/10.1002/admi.202102526 (2022).
6. Paramjot Singh, P. A. & Kahrizi, S. M. In silico design and analysis of Pt functionalized graphene-based FET sensor for COVID-19 biomarkers: A DFT coupled FEM study. *Phys. E Low-dimens. Syst. Nanostruct.* **135**, 114972 https://doi.org/10.1016/j.physe.2021.114972 (2022).
7. Wangkheirakpam, V. D., Bhowmick, B. & Pukhrambam, P. D. Detection of SARS-CoV-2 using dielectric modulated TFET-based biosensor. *J. Mater. Sci. Mater. Electron.* **33**(13), 10323–10334. https://doi.org/10.1007/s10854-022-08020-3 (2022).
8. Janik, E., Bartos, M., Niemcewicz, M., Gorniak, L. & Bijak, M. SARS-CoV-2: Outline, prevention, and decontamination. *Pathogens*. **10**(2), 114. https://doi.org/10.3390/pathogens10020114 (2021).
9. Bergmann, C. C. & Silverman, R. H.COVID-19: Coronavirus replication, pathogenesis, and therapeutic strategies. *Clevel. Clin. J. Med. Jun*. **87**(6), 321–327. https://doi.org/10.3949/ccjm.87a.20047 (2020).
10. Nasiri, K. & Dimitrova, A. Comparing saliva and nasopharyngeal swab specimens in the detection of COVID-19: A systematic review and meta-analysis. *J. Dent. Sci.* **16**(3), 799–805. https://doi.org/10.1016/j.jds.2021.01.010 (2021).
11. Nayana, G. H. & Vimala, P. Effectiveness of graphene nano-ribbon tunnel field effect transistor for bio-molecular identification. *Nano*. **18**(14), 2350113. https://doi.org/10.1142/S1793292023501138 (2023).
12. Azam, P. F. H. N., Wang, L., Kuroda, M. A., Hamilton, M. C., Hasim, S. & Mahjouri-Samani, M. Two-dimensional-material-based field-effect transistor biosensor for detecting COVID-19 virus (SARS-CoV-2). *ACS Nano*. **15**(7), 11461–11469. https://doi.org/10.1021/acsnano.1c01188 (2021).
13. Bharadwaj, D., Arpitha, N., Siddarth, M. & Usha, C. Performance snalysis of extended gate FET pH Biosensor. In *2021 IEEE International Conference on Electronics, Computing and Communication Technologies (CONECCT), Bangalore, India*, 1–5 https://doi.org/10.1109/CONECCT52877.2021.9622712 (2021).
14. Vimala, P., Saleem, S. & Samuel, A. Design and evaluation of a double-gate tunnel field effect transistor for the detection of breast cancer cells. *J. Biomimetics Biomaterials Biomedical Eng.* **64**, 105–113. https://doi.org/10.4028/p-nKu9ik (2024).
15. Fathi-Hafshejani, P. et al. *Two-Dimensional-Material-Based Field-Effect Transistor Biosensor for Detecting COVID-19 Virus (SARS-CoV-2)*, 1936-085 https://doi.org/10.1021/acsnano.1c01188 (American Chemical Society, 2021)
16. Chen, P. H., Huang, C. C., Wu, C. C., Chen, P. H. & Tripathi, A. Wang,Saliva-based COVID-19 detection: A rapid antigen test of SARS-CoV-2 nucleocapsid protein using an electrical-double-layer gated field-effect transistor-based biosensing system. *Sens. Actuators B: Chem. Volume*. **357** https://doi.org/10.1016/j.snb.2022.131415 (2022).
17. Das, B., Borah, H. & Bhowmick, B. A detailed review on growth and evolution of TFET biosensor for biosensing application. In *Handbook of Emerging Materials for Semiconductor Industry* (eds Song, Y. S. et al.) https://doi.org/10.1007/978-981-99-6649-3_43. (Springer, 2024).
18. Darshan, K. et al. Impact analysis and simulation of cylindrical nanowire biosensor. In *2021 IEEE Mysore Sub Section International Conference (MysuruCon), Hassan, India*, 285–288. https://doi.org/10.1109/MysuruCon52639.2021.9641551 (2021).
19. Kim, S. & Lee, J. H. Current advances in paper-based biosensor technologies for rapid COVID-19 diagnosis. *BioChip J.* **16**, 376–396. https://doi.org/10.1007/s13206-022-00078-9 (2022).
20. Truong, P. L., Yin, Y., Lee, D. & Ko, S. H. Advancement in COVID-19 detection using nanomaterial-based biosensors. *Exploration*. https://doi.org/10.1002/EXP.20210232 (2023).
21. Pradhan, A. et al. Biosensors as nano-analytical tools for COVID-19 detection. *Sensors*. **21**(23), 7823. https://doi.org/10.3390/s21237823 (2021). PMID: 34883826; PMCID: PMC8659776.
22. Vimala, P., Krishna, L. L. & Sharma, S. S. TFET biosensor simulation and analysis for various biomolecules. *Silicon* **14**, 7933–7938. https://doi.org/10.1007/s12633-021-01570-x (2022).
23. Piccinini, E. et. al. Biofunctionalization of Graphene-Based FET sensors through heterobifunctional nanoscaffolds: technology validation toward rapid COVID-19 diagnostics and monitoring. *Adv. Mater. Interfaces* **9**(2022).
24. Rasool, A., Kossar, S., Parveen, S. & Rasool, U. Heterojunction tunnel field-effect transistors (TFETs) and applications. In *Handbook of Emerging Materials for Semiconductor Industry* (eds Song, Y. S. et al.) https://doi.org/10.1007/978-981-99-6649-3_33. (Springer, 2024).
25. Kim, G., Lee, J., Kim, J. H. & Kim, S. High on-current Ge-channel heterojunction tunnel field-effect transistor using direct band-to-band tunneling. *Micromachines* **10**, 77. https://doi.org/10.3390/mi10020077 (2019).
26. Kong, D. et al. Direct SARS-CoV-2 nucleic acid detection by Y-shaped DNA dual-probe transistor assay. *J. Am. Chem. Soc.* **143**(41), 17004–17014 (2021).
27. Yadav, S., Gedam, A. & Tirkey, S. A dielectric modulated biosensor for SARS-CoV-2. *IEEE Sens. J.* **21**(13), 14483–14490. https://doi.org/10.1109/JSEN.2020.3019036 (2021).
28. Vanlalawmpuia, K. & Bhowmick, B. Analysis of hetero-stacked source TFET and heterostructure vertical TFET as dielectrically modulated Label-Free biosensors. *IEEE Sens. J.* **22**(1), 939–947. https://doi.org/10.1109/JSEN.2021.3128473 (2022).
29. Saha, P. & Kumar Sarkar, S. Analytical modeling of ion sensitive broken gate TFET for pH sensing applications. *IEEE Sens. Lett.* **4**(7), 1–4, Art no. 2000304. https://doi.org/10.1109/LSENS.2020.2999207 (2020).
30. Patil, M., Gedam, A. & Mishra, G. P. Performance assessment of a cavity on source charge plasma TFET-based biosensor. *IEEE Sens. J.* **21**(3), 2526–2532. https://doi.org/10.1109/JSEN.2020.3027031 (2021).
31. Dwivedi, P., Singh, R. & Chauhan, Y. S. Crossing the Nernst limit (59 mV/pH) of sensitivity through tunneling transistor-based biosensor. *IEEE Sens. J.* **21**(3), 3233–3240. https://doi.org/10.1109/JSEN.2020.3025975 (2021).
32. Kim, S. et al. Multiplexed silicon nanowire tunnel FET-based biosensors with optimized multi-sensing currents. *IEEE Sens. J.* **21**(7), 8839–8846. https://doi.org/10.1109/JSEN.2021.3054052 (2021).
33. Sakib, F. I., Hasan, M. A. & Hossain, M. Negative capacitance gate-all-around tunnel FETs for highly sensitive label-free biosensors. *IEEE Trans. Electron Devices*. **69**(1), 311–317. https://doi.org/10.1109/TED.2021.3129711 (2022).

34. Shafi, N., Sahu, C., Periasamy, C. & Singh, J. SiGe source charge plasma TFET for biosensing applications. In *Nanoelectronic and Information Systems (iNIS). 2017 IEEE International Symposium*, 93–98 (2017).
35. Bind, M. K., Singh, S. V. & Nigam, K. K. Design and performance evaluation of a heterojunction GaAs/GaSb PC-TFET for label-free biosensing applications, *J. Electron. Mater.* **54**(4), 1691–1708 https://doi.org/10.1007/s11664-024-11643-3 (2025).
36. Choi, W. Y., Park, B.-G., Lee, J. D. & Liu, T.-J. K. Tunneling field-effect transistors (TFETs) with subthreshold swing (SS) less than 60 Mv/Dec. *IEEE Electron. Device Let*. **28**(8), 743 (2017).

Author contributions

P.Vimala: Conceptualization, Methodology, Software, Data curation, Formal analysis, Investigation, Resources, VisualizationA. Sharon Geege: Implementation, Validation, and Writing-original draft preparation.N.Mohankumar: Conceptualization, Methodology, Supervision, Writing-original draft preparation and Resources.T.S. Arun Samuel: Data curation, Funding, Validation, VisualizationT. Ananth Kumar: Validation, Methodology, software, and Writing-original draft preparation.P.Suveetha Dhanaselvam: Formal analysis, Writing – review & editing.I.Vivek Anand: Visualization, and Writing-review and editing.

Declarations

Competing interests

The authors declare no competing interests.

Additional information

Correspondence and requests for materials should be addressed to P.V. or T.A.K.

Reprints and permissions information is available at www.nature.com/reprints.

Publisher's note Springer Nature remains neutral with regard to jurisdictional claims in published maps and institutional affiliations.